Human Molecular Genetics, 2012, Vol. 21, No. 3 **577–585**
doi:10.1093/hmg/ddr493
Advance Access published on October 28, 2011

A novel mutation within the *MIR96* gene causes non-syndromic inherited hearing loss in an Italian family by altering pre-miRNA processing

Giulia Soldà[1,*], Michela Robusto[1], Paola Primignani[3], Pierangela Castorina[4], Elena Benzoni[3], Antonio Cesarani[2,4], Umberto Ambrosetti[2,4], Rosanna Asselta[1] and Stefano Duga[1]

[1]Dipartimento di Biologia e Genetica per le Scienze Mediche and [2]Dipartimento di Scienze Chirurgiche Specialistiche, Università degli Studi di Milano, Milan, Italy, [3]Medical Genetics Laboratory and [4]UO Audiology, Fondazione IRCCS Cà Granda, Ospedale Maggiore Policlinico, Mangiagalli e Regina Elena, Milan, Italy

Received August 2, 2011; Revised and Accepted October 23, 2011

The miR-96, miR-182 and miR-183 microRNA (miRNA) family is essential for differentiation and function of the vertebrate inner ear. Recently, point mutations within the seed region of miR-96 were reported in two Spanish families with autosomal dominant non-syndromic sensorineural hearing loss (NSHL) and in a mouse model of NSHL. We screened 882 NSHL patients and 836 normal-hearing Italian controls and identified one putative novel mutation within the miR-96 gene in a family with autosomal dominant NSHL. Although located outside the mature miR-96 sequence, the detected variant replaces a highly conserved nucleotide within the companion miR-96*, and is predicted to reduce the stability of the pre-miRNA hairpin. To evaluate the effect of the detected mutation on miR-96/mir-96* biogenesis, we investigated the maturation of miR-96 by transient expression in mammalian cells, followed by real-time reverse-transcription polymerase chain reaction (PCR). We found that both miR-96 and miR-96* levels were significantly reduced in the mutant, whereas the precursor levels were unaffected. Moreover, miR-96 and miR-96* expression levels could be restored by a compensatory mutation that reconstitutes the secondary structure of the pre-miR-96 hairpin, demonstrating that the mutation hinders precursor processing, probably interfering with Dicer cleavage. Finally, even though the mature miR-96 sequence is not altered, we demonstrated that the identified mutation significantly impacts on miR-96 regulation of selected targets. In conclusion, we provide further evidence of the involvement of miR-96 mutations in human deafness and demonstrate that a quantitative defect of this miRNA may contribute to NSHL.

INTRODUCTION

MicroRNAs (miRNAs) are ~21-nucleotide (nt)-long, single-stranded noncoding RNAs that mainly function as post-transcriptional regulators of gene expression. Once assembled into an RNA-induced silencing complex, each miRNA might inhibit the expression of hundreds of target messenger RNAs (mRNAs), by inducing translational repression and/or mRNA degradation (1). Animal miRNAs recognize partially complementary binding sites, which are generally located in the 3′ untranslated region (3′UTR) of target mRNAs. In particular, complementarity to the miRNA seed region, corresponding to nts 2–8 at the 5′ of the mature miRNA, is a major determinant in target recognition and is sufficient to trigger silencing (2).

MiRNAs are initially transcribed from endogenous genes as long primary transcripts (pri-miRNAs), which contain extended hairpin structures. The pri-miRNAs are then processed by the Microprocessor complex into a hairpin precursor (pre-miRNA), which is exported to the cytoplasm and cleaved by the RNaseIII Dicer to generate a mature miRNA duplex (3). Usually, one strand of the duplex is preferentially selected for entry into the silencing complex to regulate gene expression, whereas the other strand, known as the passenger

*To whom correspondence should be address at: Department of Biology and Genetics for Medical Sciences, Via Viotti 3/5, 20133, Milan, Italy. Tel: +39 0250315852; Fax: +39 0250315864; Email: giulia.solda@unimi.it

strand or miRNA*, has typically been assumed to be degraded. However, recent evidence demonstrated that miRNA* species are often present at physiologically relevant levels, can associate with the silencing protein Argonaute and can inhibit target mRNAs in both cultured cells and transgenic animals (4–8).

The miR-183 family is composed of three miRNAs (miR-183, miR-96 and miR-182), which are coordinately expressed from a single genetic *locus* in vertebrates. Homologous miRNAs (miR-228 and mir-263b) are also present in invertebrates (9). Importantly, this highly conserved family of miRNAs shows expression in ciliated neurosensory organs across *phyla* and has recently been demonstrated to contribute specifically to the differentiation and function of the mechanosensory hair cells in the vertebrate inner ear (10,11). For instance, in zebrafish, the miR-183 family is predominantly expressed in the hair cells of the inner ear and of the lateral line, as well as in the olfactory and retinal sensory cells (12,13). Overexpression of miR-96 or miR-182, but not of miR-183, was shown to induce duplicated otocysts, ectopic or expanded sensory patches, and extra hair cells. Conversely, knockdown of each of the three miRNAs led to a reduction in the number of hair cells in the inner ear and caused defects in semicircular canals, as well as the presence of abnormal neuromasts in the lateral line (11).

In the human genome, the miR-183 family is clustered in a 4.5 kb region on chromosome 7q32, within a *locus* that has been linked to autosomal dominant non-syndromic hearing loss (NSHL) (DFNA50, OMIM #613074). In 2009, two mutations in the seed region of miR-96 were detected in two Spanish families affected by autosomal dominant progressive NSHL. Both mutations (+13G>A and +14C>A) affect nts that are fully conserved among vertebrates (from fish to humans) and segregated with hearing loss in the affected families. The impact of these mutations on miR-96 processing and target recognition was analyzed in HeLa and NIH-3T3 cells, showing that both mutations result in reduced levels of mature miRNA and hinder its gene-silencing capacity (14). Further evidence on the significance of miR-96 expression and function in the pathogenesis of hearing loss has been provided by genetic studies in the mouse, where a single nt substitution in the seed region of the homolog of miR-96 was shown to cause progressive hearing loss and hair cell defects in a murine model of sensorineural deafness, called diminuendo (15,16). The work of Mencía *et al*. (14) represented the first evidence that point mutations in a miRNA can be responsible for a Mendelian trait. However, up to now, the mutational screening of the miR-183 family has been performed only in the original study—including 567 Spanish families with inherited hearing loss (14)—and in a single replication study on 150 American families with autosomal dominant NSHL, where no mutations were found (17). Therefore, a positive replication of the findings by Mencía *et al*. is still lacking.

In this study, we have identified a novel NSHL-causing mutation within the *MIR96* gene by screening a large case–control Italian population. At variance with previously reported mutations, this variation does not affect the miR-96 seed region, but alters the companion miR-96* sequence. Through a series of functional studies, we have demonstrated that this variant substantially impairs the production of mature miR-96 by altering the pre-miRNA secondary structure, and indirectly impacts on the normal regulation of miR-96 targets. Our results suggest that a quantitative defect of miR-96 can be sufficient to cause deafness. However, as we have shown that the novel mutation also reduces the expression levels of miR-96* and potentially alters the recognition of its targets, a contribution of this miRNA species to NSHL pathogenesis cannot be ruled out.

RESULTS

A novel NSHL-causing mutation within the *MIR96* gene

A cohort composed of 882 genetically undiagnosed Italian NSHL patients, including sporadic and familial cases, and 836 normal-hearing Italian controls was screened for mutations in miR-96, miR-182 and miR-183 genes. A strategy based on a prescreening by high-resolution melting (HRM) followed by direct sequencing was chosen. Neither of the two previously reported miR-96 mutations was found, suggesting that they might represent private mutations. Instead, five heterozygous nt variations were identified in NSHL cases (Supplementary Material, Table S1): two of them, miR-96(+42C>T) and miR-182 (+106G>A), were previously reported as single nt polymorphisms (SNPs rs73159662 and rs76481776, respectively), and were found also in controls. Two novel *MIR183* variants, miR-183(+3G>T) and miR-183(-27C>T), were detected, each in one proband: both were located outside the mature miRNA sequence at non-conserved nt residues, were absent in normal-hearing controls, but did not segregate with hearing loss in the corresponding families (the variants were absent in at least one affected relative in the corresponding family). The last variant identified, miR-96(+57T>C) (NR_029512.1:c.57T>C; NT_007933.15:g.67447397A>G) is located in the stem region of the pre-miRNA and replaces a residue that is fully conserved throughout vertebrate evolution, from fish to primates (Fig. 1A). This variation affects the mature miR-96*, which is processed from the complementary strand of the miR-96 precursor. In particular, the change occurs at position +6, within the miR-96* seed region (Fig. 1A). The miR-96* has been experimentally detected in humans, mouse, platypus and zebrafish (mirBase, http://www.mirbase.org/) (18), suggesting that also the miRNA* species has been maintained throughout vertebrate evolution, although its sequence is only partially conserved. However, very little is known about miR-96* expression and function.

The miR-96(+57T>C) mutation was found in the heterozygous state in a patient with a family history of autosomal dominant progressive NSHL (with the age of onset ranging from ~25 to 40) and was absent in all 839 normal-hearing controls. The proband is a profoundly deaf 56-year-old woman with an affected brother, two normal hearing sisters and three normal-hearing children (Fig. 1B and C). The proband's mother and grandmother were also profoundly deaf, but with a various degree of hearing loss (the grandmother being slightly more severe; Supplementary Material, Fig. S1). The proband shows non-syndromic, bilateral, sensorineural deafness that onset as a mild hearing impairment at ~25 years and slowly progressed first to a severe form at the age of 45 and then to a profound form in the sixth decade (Fig. 1D). She presents a down-sloping audiometric

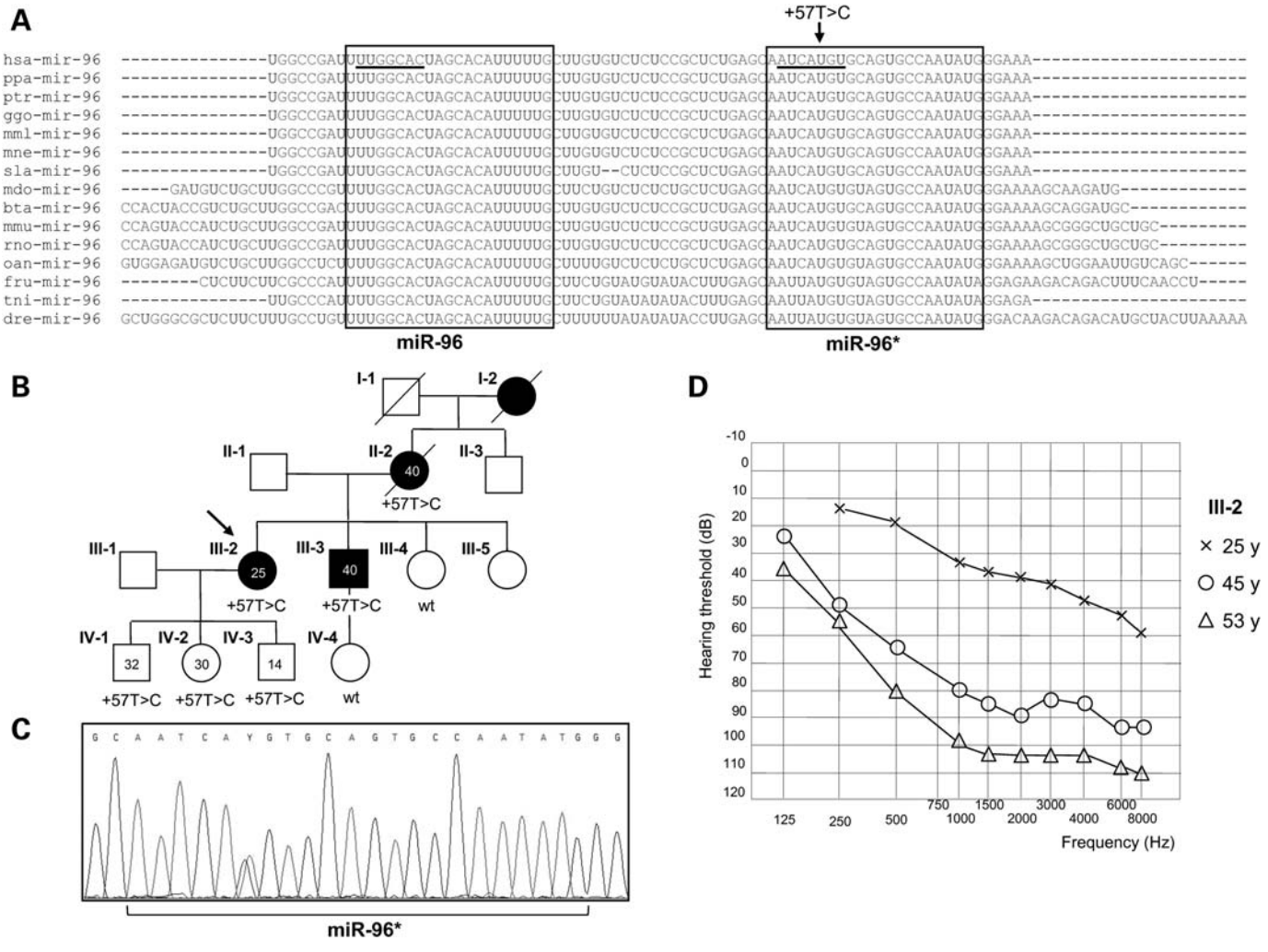

Figure 1. The novel pre-miR-96(+57T>C) mutation identified in an Italian family with autosomal dominant non-syndromic hearing loss. (**A**) Multiple alignment of pre-miR-96 sequences (annotated in miRBase) from different vertebrate species obtained using the CLUSTALW software. The nt position +57 within the human pre-miR-96 is indicated by an arrow. Mature miR-96 and miR-96* sequences are boxed, and their seed regions are underlined. hsa, *Homo sapiens*; ppa, *Pan paniscus*; ptr, *Pan troglodytes*; ggo, *Gorilla gorilla*; mml, *Macaca mulatta*; mne, *Macaca nemestrina*; sla, *Saguinus labiatus*; mdo, *Monodelphis domestica*; bta, *Bos taurus*; mmu, *Mus musculus*; rno, *Rattus norvegicus*; oan, *Ornithorhynchus anatinus;* fru, *Fugu rubipres*; tni, *Tetraodon nigroviridis*; dre, *Danio rerio*. (**B**) Pedigree of the Italian NSHL family carrying the miR-96(+57T>C) mutation. Black symbols indicate affected subjects. The numbers within the symbols represent: age of onset of NSHL (black symbols) and present age (empty symbols). Presence or absence of the mutation is indicated below the genetically analyzed subjects. (**C**) Electropherogram depicting the pre-miR-96 sequence surrounding the mutated nt. (**D**) Audiograms showing the progression of the hearing impairment in the proband (III-2). The age at which each audiometric record was obtained is indicated. Each graph point represents the average hearing loss for the right and left ears.

profile in which all frequencies are affected (Fig. 1D). Neither the proband nor any affected individuals of her family referred visual or olfactory problems; however, episodes of vertigo were reported in the proband (III-2), her mother (II-2) and her brother (III-3). The miR-96(+57T>C) variant segregates with the phenotype within the family, being present in all affected individuals and absent in the normal hearing individuals III-4 and IV-4. However, the variation is also present in the three normal-hearing proband's children (Fig. 1C and Supplementary Material, Fig. S1): this may be due either to the age-relatedness of hearing loss in the family (all non-penetrants are below the average age of onset of the disease among affected relatives) or to incomplete penetrance.

The +57T>C mutation impairs pre-miRNA processing into mature miR-96 and miR-96*

As the miR-96(+57T>C) variation is located in the stem region of the miRNA precursor, we used the mfold program (19) to examine how the newly identified nt variation could alter the predicted RNA secondary structure of pre-miR-96. The miR-96(+57T>C) substitution introduces a base-pairing mismatch, decreasing the free energy value and creating an enlarged RNA bulge in the pre-miR-96 stem, close to the Dicer cleavage site (Fig. 2A). In this frame, we decided to examine the impact of the novel variant on both miR-96 and miR-96* expression and maturation. To this aim, expression vectors (psiUX) containing genomic DNA fragments spanning both miR-183 and miR-96

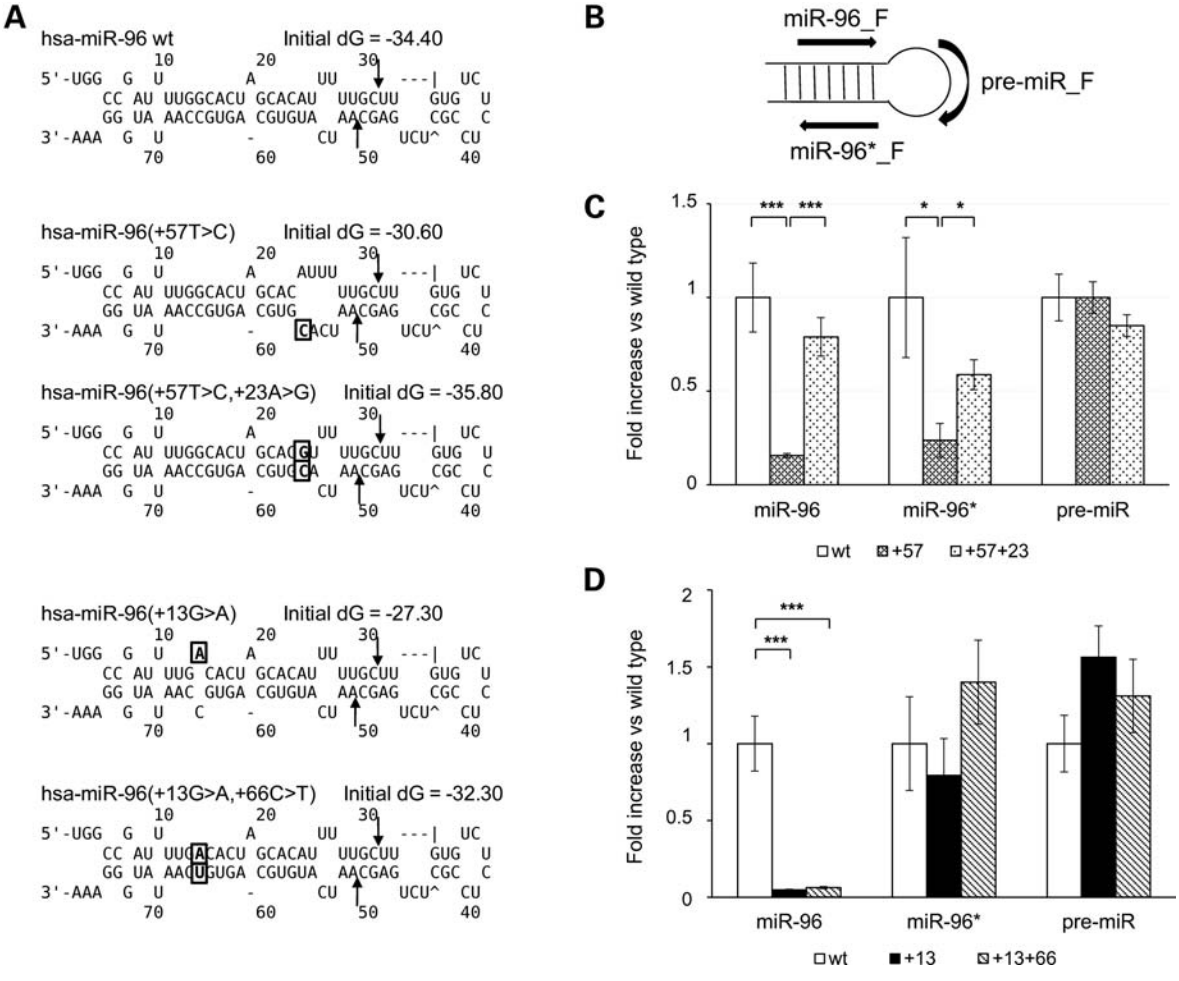

Figure 2. Different functional consequences of the miR-96(+57T>C) and the known miR-96(+13G>A) mutations on miR-96/miR-96* biogenesis. (**A**) Predicted secondary structures of wild-type, mutant (+57T>C and +13G>A) and double-mutant (+23A>G+57T>C and +13G>A+66C>T) miR-96 precursors obtained by using the mfold algorithm. The nt positions involved in the mutations are boxed. The double mutants were created to restore the pre-miR-96 secondary structure, in order to verify whether the defects in miRNA expression were dependent on correct folding of the hairpin precursor. Dicer cleavage sites are indicated by arrows. (**B**) The positions of the 5′ primers used for real-time RT–PCR to quantify the levels of mature miRNA and pre-miRNA species. Primer sequences are listed in Supplementary Material, Table S2. (**C**) The miR96(+57T>C) impairs the processing of pre-miR-96 to its mature forms, and is rescued by a compensatory mutation (+23A>G) restoring the correct hairpin folding. (**D**) The known miR96(+13G>A) impairs mature miR-96, but not miR-96* levels, independently from the correct folding of the miR-96 precursor. The effect of the analyzed mutants on pre-miR-96 processing was evaluated by quantitative real-time RT–PCR using the △△CT method. Variations in the expression levels of mature miRNAs and pre-miR-96 in the miR-96(+57T>C) and miR-96(+23A>G+57T>C) (C), or the known miR-96(+13G>A) and miR-96(+13G>A+66C>T) (D) mutants were compared with the wild-type samples (set as 1). Bars stand for mean ± SEM (represented as percentage of variation) of six independent experiments, each performed in triplicate in different days on different cell batches and with different plasmid preparations. The results were analyzed by unpaired *t*-test ($^{*}P < 0.05$; $^{**}P < 0.01$; $^{***}P < 0.001$).

precursors, and corresponding to either the miR-96 wild-type or the miR-96(+57T>C) sequences, were generated and used to transiently transfect HeLa cells. Total RNA was extracted 24 h after transfection, reverse transcribed and the expression levels of mature miR-96, miR-96* as well as of pre-miR-96 were evaluated by real-time reverse-transcription polymerase chain reaction (RT–PCR), with specific custom-designed assays (Fig. 2B). Standard curves were generated to verify that the RT–PCR assays had comparable amplification efficiencies (see Materials and Methods and Supplementary Material, Fig. S2). In all experiments, miR-183 was used as internal control to normalize for transfection efficiency. Interestingly, expression levels of both miR-96 and miR-96* were significantly reduced in the mutant (+57T>C) compared with the wild-type (85% reduction, $P = 0.0006$ for miR-96 and 77% reduction, $P = 0.019$, for miR-96*, respectively), whereas the precursor levels were unaffected by the mutation (Fig. 2C). Similar experiments were performed using a third expression vector carrying one of the known miR-96 mutations (+13G>A), previously shown, by Northern blot experiments, to decrease the level of miR-96 (14). In this case, the mutant showed a significant reduction in mature miR-96 ($P < 0.0001$) but, unexpectedly, miR-96* levels were unaffected (Fig. 2D), suggesting an at least partially different pathogenic mechanism.

The same approach was used to verify whether presumably non-pathogenic variants within *MIR96* impact the normal levels of the mature miRNA. Hence, we selected the two known polymorphisms within *MIR96* that are currently

annotated in dbSNP (rs73159662, +42C>T; and rs41274239, +36T>C). Both are located within the loop region of the miR-96 precursor, and were detected in the heterozygous state in healthy controls during our genetic screening (Supplementary Material, Fig. S3 and Table S1). No significant alteration of miR-96, miR-96* and pre-miR-96 levels was measured by real-time RT–PCR, although the rs73159662 mutant tends to produce slightly elevated levels of both mature miRNA species (Supplementary Material, Fig. S3).

The miR-96(+57T>C) mutation is rescued by reconstituting the precursor secondary structure

The miR-96(+57T>C) mutation causes a reduction in both mature miRNAs but does not alter the expression level of the miRNA precursor, thus suggesting a defect in the Dicer-mediated cleavage.

This may be due to the modification of the normal pre-miR-96 secondary structure close to the Dicer cleavage site, as predicted by mfold (see above and Fig. 2A). If this is true, a second mutation that would reconstitute the pairing of the +57 nt and hence the physiologic secondary structure of the miR-96 precursor (Fig. 2A) should restore miR-96 and miR-96* levels. To verify this hypothesis, we transfected HeLa cells with the double-mutant vector psiUX-miR-96(+23 A>G+57T>C), and evaluated the expression levels of miR-96, miR-96* and pre-miR-96. Both miR-96 and miR-96* levels were significantly increased in the double mutant compared with the +57T>C mutant ($P = 0.0003$ and $P = 0.02$, respectively) restoring mature miRNA expression at levels not significantly different from the wild-type (Fig. 2C). These results confirm that reduced miR-96/miR-96* levels, caused by the miR-96(+57T>C) mutation, are a consequence of the altered precursor secondary structure.

As comparison, we next verified if also the effect of the known miR-96(+13G>A) mutation could be rescued by restoring the correct folding of the miR-96 precursor. In principle, as this mutation does not impair the precursor expression and affects only one of the mature miRNA species (Fig. 2D), it should not directly interfere with either the Microprocessor-mediated or the Dicer-mediated cleavage steps. Indeed, transfection of a double-mutant vector carrying a compensatory mutation, psiUX-miR-96(+13G>A+66C>T), confirmed this hypothesis: miR-96 levels were still markedly reduced in the double mutant compared with the wild-type ($P < 0.0001$), and not significantly different from the +13G>A mutant, whereas the miR-96* and pre-miRNA levels remained unaffected (Fig. 2D). These results indicate that the known +13G>A mutation reduces mature miR-96 levels in a way that is independent from the correct folding of the hairpin precursor, pointing again to different pathogenic mechanisms for the +13G>A and the +57T>C mutations.

Impact of the +57T>C mutation on miRNA target regulation

We next evaluated the effect of the miR-96(+57T>C) mutation on the regulation of both miR-96 and miR-96* mRNA targets by luciferase reporter assays. First, we selected eight candidate target genes that: (i) contained either a 7-nt perfect match or multiple 6-nt binding sites for the miR-96* and/or for the miR-96 seed region; (ii) were predicted as potential miR-96/miR-96* targets by several bioinformatics programs (i.e. PITA, RNAhybrid, miRANDA/mirSVR) (20–22); (iii) were reported in the literature to be expressed in the vertebrate inner ear/auditory system (see below—Materials and Methods). Three of them (*ACVR2B*, *CACNB4* and *MYRIP*) were predicted as common miR-96/miR-96* targets, whereas the other five (*ALCAM*, *BBS4*, *IQGAP2, PLS3* and *ROCK2*) were targets of the miR-96* only (Supplementary Material, Fig. S4). To validate the candidate targets, we co-transfected a vector expressing either the wild-type or the mutant pre-miR-96 hairpin into HeLa cells, together with a construct containing the luciferase reporter cDNA coupled to the 3′UTR of each target gene (psiCHECK2-3′UTR). This reporter system showed that three (*MYRIP*, *ACVR2B*, *CACNB4*) out of eight luciferase-3′UTR constructs were controlled by human miR-96/miR-96* and that the miR-96(+57T>C) mutation led, in all cases, to a significantly reduced silencing (~50%) of luciferase expression compared with the wild-type pre-miR-96 (Fig. 3A and Supplementary Material, Fig. S5). In particular, the *MYRIP* 3′UTR, which contains an already validated miR-96 target site (14) as well as a predicted miR-96* site, showed the most significant regulation. To discriminate between the relative effect of miR-96 and miR-96* on *MYRIP* 3′UTR regulation, we created two mutant 3′UTR constructs in which the miR-96 or the miR-96* binding sites were selectively disrupted. While the construct lacking the miR-96*-binding site was still significantly responsive to miR-96 repression ($P < 0.01$), the mutant deprived of miR-96-binding site was not (Fig. 3A), indicating that *MYRIP* 3′UTR is regulated uniquely by miR-96, and that the predicted miR-96* binding site is not functional. Therefore, the impaired regulation of *MYRIP* 3′UTR in the miR-96(+57T>C) mutant is likely a consequence of the reduced levels of miR-96, caused by the defect in the hairpin processing. To confirm this hypothesis, we repeated the luciferase assays using the double miR-96(+23 A>G+57T>C) mutant, and observed that in this case the downregulation of *MYRIP* 3′UTR was restored to a level similar to that of the wild-type miR-96 (Fig. 3B). Hence, we can conclude that a quantitative defect in miR-96 production might be sufficient to impair the regulation of at least some of its downstream targets.

DISCUSSION

Here we report a novel mutation within the *MIR96* gene that causes autosomal dominant post-lingual progressive NSHL in an Italian family. This is the third mutation described in this gene in humans, and the first in a different population from that of the original report (14). The +57(T>C) variant is also the first mutation in the *MIR96* gene that does not affect the miR-96 seed region, neither its mature sequence. Instead, our results indicate that this mutation alters the correct maturation of the precursor miR-96, leading to a decrease in the level of both its mature forms. In particular, the +57(T>C) mutation is predicted to create an enlarge bulge in the secondary structure of miR-96 hairpin, 5 nts 3′

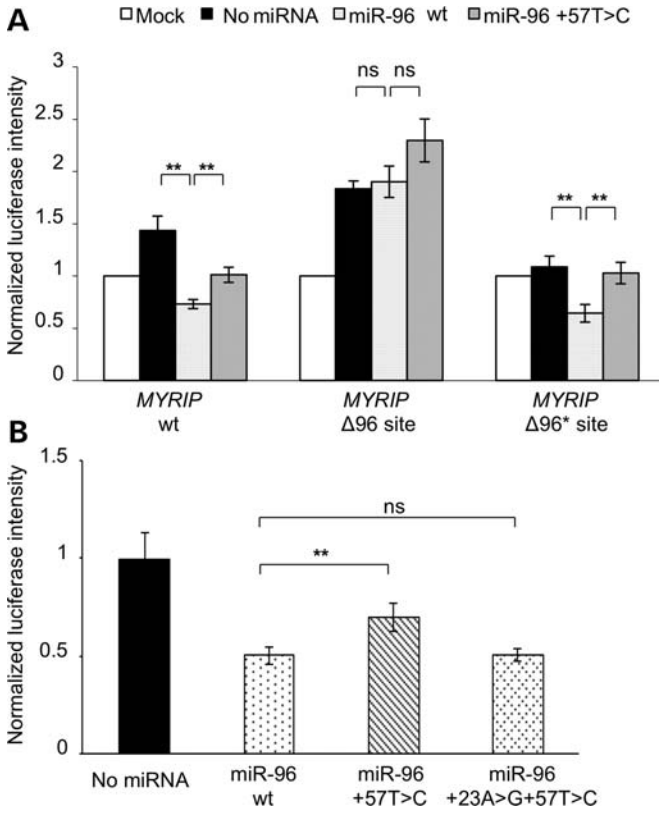

Figure 3. The miR96(+57T>C) mutation impairs the regulation of *MYRIP* by reducing mature miR-96 levels. (**A**) Downregulation of *MYRIP* 3′UTR is only dependent on miR-96, and is impaired in the miR96(+57T>C) mutant. The *MYRIP* 3′UTR reporter vectors (wild-type, or Δ96 and Δ96* mutants) were cotransfected with plasmids expressing either the wild-type or the +57T>C mutant pre-miR-96. Mock samples were transfected with the empty psiCHECK2 and psiUX vectors. (**B**) Restoration of correct pre-miR-96 folding rescues the regulation of *MYRIP* 3′UTR. The wild-type *MYRIP* 3′UTR reporter vector was cotransfected with the wild-type, the +57T>C or the double-mutant (+23A>G+57T>C) pre-miR-96 expression constructs. Relative luciferase activity is expressed as mean ± SEM of six independent experiments, each performed in triplicate in different days on different cell batches and with different plasmid preparations. The luciferase activity of the empty psiCHECK2 plasmid (A) or of the corresponding psiCHECK2-3′UTR plasmid (B) is set as 1. The results were analyzed by unpaired *t*-test ($^{*}P < 0.05$; $^{**}P < 0.01$; $^{***}P < 0.001$).

to the Dicer cleavage site (Fig. 2A), suggesting that it might interfere with Dicer processing. Other studies have reported that common SNPs within miRNA genes can lead to impaired miRNA processing, and might be associated with increased susceptibility to human diseases (23–25). Interestingly, one SNP within the miR-146a, which confers an increased risk to develop thyroid cancer, not only hindered the pre-miRNA processing, but also affected the seed region of the companion miR-146a*, similarly to the miR-96(+57T>C) mutation. The miR-146a* was expressed in both normal and tumor thyroid tissues and the altered regulation of the miRNA* targets in heterozygotes compared with homozygotes was suggested as the possible mechanism underlying tumor predisposition (26).

In the case of the miR-96(+57T>C) mutation, however, a direct role of miR-96* in NSHL pathogenesis has still to be proved. In fact, none of the putative miR-96* target sites was validated by luciferase-based assays (Supplementary Material, Fig. S5). Profiling of miR-96* expression in a panel of human and mouse tissues evidenced that, although expressed at very low levels, miR-96* shows some degree of differential expression, suggesting that it might be regulated in a tissue-specific manner (Supplementary Material, Fig. S6). In the mouse Organ of Corti, the miR-96* could be cloned, but not reliably quantitated by real-time RT–PCR. More extensive and detailed experiments will be needed to define the role, if any, of this miRNA* species in the inner ear, as well as to evaluate the involvement of the mutant miR-96* in NSHL.

Even though mutations within miR-96 are not a common cause of deafness, as evidenced by this and previous works (14,17), the description of novel causative variants might help in elucidating the pathogenic mechanisms underlying the DFNA50-associated phenotype. In particular, the functional analysis of the +57(T>C) mutation points to a contribution of quantitative defects in miR-96 to hearing loss pathogenesis, independently from additional qualitative defects (i.e. changes in the actual mature miR-96 sequence). Indeed, tight regulation of miR-96 levels within the vertebrate inner ear seems to be crucial for the correct function and development of hair cells, as demonstrated by knockdown experiments in zebrafish (11) and by the phenotypic differences between the heterozygous and the homozygous diminuendo mice (15,16). Interestingly, also the three affected families (the two Spanish and the here reported Italian one) show some degree of phenotypic variation, suggesting that the pathogenic mechanisms underlying each family's phenotype might be at least partially different. In particular, the family carrying the +57(T>C) mutation is characterized by a late onset (between 25 and 40 years) and a slow progression of the hearing impairment. In addition, the presence of the mutation in three young individuals of the last generation (Fig. 1B), who currently have normal hearing at audiological analysis (Supplementary Material, Fig. S1), suggests incomplete penetrance, although they might still develop the disease in the future. The phenotypic differences with the previously reported families might be partly explained by molecular findings: a quantitative defect of miR-96 expression may lead to a delayed or reduced penetrance of the hearing impairment, whereas mutations directly impairing miR-96 target recognition would probably result in an earlier defect of hearing. In this respect, it should be recalled that the *diminuendo* mouse, which carries a mutant miR-96 seed region, does not have a major effect on miR-96 expression levels (15).

In conclusion, deciphering the different pathogenic mechanisms linking *MIR96* mutations to progressive hearing loss will be crucial for helping to develop new personalized therapeutic approaches for people carrying these mutations.

MATERIALS AND METHODS

Patients selection

This study was approved by the local Ethical Committee of the University of Milan and was performed according to the Declaration of Helsinki and to the Italian legislation on sensible data recording. Signed informed consent was obtained from all participants and from parents of subjects younger than

18 years. Clinical history ruled out environmental factors as cause of the hearing loss and physical examination did not reveal any evidence of syndromic features.

A total of 882 genetically undiagnosed NSHL patients (familial 30%, and sporadic 70%) were recruited. All patients underwent ear, nose and throat, and audiological examinations. For adults and collaborative children, hearing levels were determined by pure-tone audiometry, in accordance with International Standard Organization (ISI 8253-1-3) protocols. The hearing impairment diagnosis of small children (<1 year) was obtained through the auditory brainstem responses and the observation of their behaviors, whereas in older children a behavioral audiometry was performed. In addition, evoked otoacoustic emissions and tympanometry with acoustic reflex thresholds were evaluated. Average thresholds in the range of 21–40 dB were defined as mild, 41–70 dB as moderate, 71–95 dB as severe and >95 dB as profound hearing loss. Finally, specific questions were asked to evaluate olfactory, visual and vestibular functions.

All recruited patients did not carry mutations within gap-junction proteins connexins 26 and 30 (*GJB2*, *GJB6*), and the mitochondrial 12S rRNA (*MTRNR1*) genes.

A total of 120 individuals with no familiarity for hearing loss and instrumentally verified normal auditory function (mean age at withdrawal 32 ± 9) were also collected as controls. Additional 716 controls with a mean age >50 years and declared normal auditory function were also recruited.

Mutational screening

Genomic DNA extraction from peripheral blood was performed using a semi-automatic extractor (Fujifilm Europe GmbH, Düsseldorf, Germany), whereas DNA from buccal swabs from small children was purified according to the QIAamp DNA Mini Kit extraction protocol (Qiagen, Hilden, Germany). DNA samples were quantified on a Nanodrop ND-1000 spectrophotometer (NanoDrop Technologies, Wilmington, DE, USA), standardized for concentration, arrayed into 96-well plates and stored at −20°C.

Although both previously reported miR-96 mutations were found in families with autosomal dominant NSHL, we chose to perform the mutational screening on all available genetically undiagnosed NSHL patients, independently from the mode of inheritance. Three sets of primer pairs were designed to PCR amplify the genomic DNA fragments containing the precursor sequences and flanking regions of *MIR183*, *MIR96* and *MIR182* (Supplementary Material, Table S1). PCR amplimers were screened for mutations by HRM on a LigthCycler 480 using the HRM Master kit (Roche, Basel, Switzerland) and a touch-down protocol (thermal profiles are available on request). Amplicons were analyzed with the Gene Scanning Software (Roche). Samples showing a melting profile different from the wild-type control were further analyzed by direct sequencing, using the BigDye Terminator Cycle Sequencing Ready Reaction Kit v1.1 (Applied Biosystems, Foster City, CA, USA) and an ABI-3130XL sequencer, as previously described (27). The Variant Reporter software was used for mutation detection (Applied Biosystems).

Computational methods

The mfold program (19) was used to evaluate the possible impact of the +57T>C mutation on the secondary structure of pre-miR-96.

We used the TargetRank program (28) to predict potential miR-96, miR-96*T (wild-type), and miR-96*C (mutant) targets and selected those genes that were either potential targets of the wild-type miR-96* only, or targeted by both the miR-96 and the wild-type miR-96*, but not the mutant miR96*. Among these, we then selected for validation by luciferase assays eight genes that: (i) contained either a 7-nt perfect match or multiple 6-nt binding sites for the miR-96* and/or miR-96 seed region; (ii) were predicted as potential miR-96/miR-96*T targets by additional bioinformatics programs (i.e. PITA, RNAhybrid, miRANDA/mirSVR) (20–22); (iii) were expressed in the inner ear/auditory system (15,29–34).

Expression vectors

To generate vectors for miRNA expression, genomic DNA fragments including both the miR-183 and the miR-96 precursors, and corresponding to either the miR-96 wild-type or the miR-96(+57T>C) sequences, were amplified from genomic DNA using modified primers (containing a *Kpn*I or a *Xho*I site at their 5′ends; Supplementary Material, Table S2), inserted into the psiUX vector (kindly provided by prof. I. Bozzoni, Università di Roma La Sapienza) (35) and then verified by sequencing. The psiUX-miR-96(+13G>A) vector, carrying one of the known miR-96 mutations (14), the double mutants, psiUX-miR-96(+23A>G+57T>C) and psiUX-miR-96(+13G>A+66C>T) and the vectors carrying the two known *MIR96* polymorphisms (rs73159662, +42C>T; and rs41274239, +36T>C) were obtained by site-directed mutagenesis using the QuikChange kit (Stratagene, La Jolla, CA, USA), following the manufacturer's instructions.

The entire 3′UTRs of putative target genes were amplified from genomic DNA and directionally cloned into a psiCHECK2 vector (Promega, Madison, WI, USA), downstream of the renilla luciferase gene. Constructs carrying mutant versions of miRNA binding sites (Δ96 and Δ96* binding sites) were obtained by site-directed mutagenesis.

Ex-vivo analysis of miRNA expression and biogenesis

HeLa cells were cultured in Dulbecco's modified Eagle medium containing 2 mM L-glutamine, 10% fetal bovine serum and antibiotics (100 U/ml penicillin and 100 μg/ml streptomycin; Euroclone, Wetherby, UK) and grown at 37°C in a humidified atmosphere of 5% CO_2 and 95% air, according to the standard procedures.

In each transfection experiment, an equal number of cells (250 000) were transiently transfected in six-well plates with the Fugene HD reagent (Promega) and 4 μg of plasmid DNA, following the manufacturer's instructions. Twenty-four hours after transfection, cells were washed twice with phosphate-buffered saline and total RNA was extracted using the EUROzol reagent (Euroclone), according to the manufacturer's instructions. RNA concentration was quantified by Nanodrop ND-1000 spectrophotometer (NanoDrop

Technologies). The miRNA First Strand Synthesis kit (Agilent Technologies, Palo Alto, CA, USA) was used to reverse transcribe miRNAs, starting from 300 ng of total RNA, according to the manufacturer's instructions. An aliquot (1 μl) of a 1:5 dilution of the RT reaction was used as template in a standard real-time RT–PCR amplification, using the universal reverse primer (Agilent Technologies) and miRNA-specific forward primers (Supplementary Material, Table S2). Although in principle the primers for the amplification of mature miR-96 and miR-96* can also amplify the pre-miRNA, real-time RT–PCR conditions were set up to favor the amplification of the mature forms and the analysis of melting curves confirmed the presence of a single amplification product (data not shown). The specific 5′ primer used to amplify mature miR-96* was designed downstream of the +57 nt position, so that the same primer could be used to amplify both the wild-type and the +57T>C mutant. Conversely, standard curves were generated to verify that the RT–PCR assays to detect: (i) wild-type miR-96, miR-96(+13G>A) or miR-96(+23A>G); (ii) wild-type miR-96* and miR-96*(+66 T>C); (iii) wild-type pre-miR-96, pre-miR-96(+42C>T) and pre-miR-96(+36T>C) had comparable amplification efficiencies (Supplementary Material, Fig. S2). In all cases, real-time RT–PCR assays were performed in triplicate on a LightCycler 480 (Roche), using a touch-down thermal profile (PCR conditions are available on request). MiRNA expression levels were quantified by the △△CT method (36) using the miR-183, co-expressed by the same construct, as internal normalization reference. An unpaired, one-tailed *t*-test was performed to test for significant differences between the mutants and the wild-type samples.

MiRNA target validation by luciferase assays

Transient transfections were performed by using the Fugene HD reagent (Roche) and 2 μg of psiCHECK2-3′UTR constructs together with 0.2 μg of the wild-type, the mutant (+57T>C) or the double-mutant (+23A>G+57T>C) psiUX-miR-96 vector. In this case, the psiUX constructs used for miRNA expression contained only the miR-96 precursor, thus avoiding the confounding effect of cloning the related miR-183. Cells co-transfected with the empty psiCHECK2 and psiUX vectors served as mocks. Forty-eight hours post-transfection, renilla and firefly luciferase activities were measured in cell lysates using the Dual-Luciferase Assay System (Promega) on a Wallac Victor 1420 Reader (Perkin Elmer Life Sciences, Waltham, MA, USA). The results were analyzed by unpaired *t*-test.

MiRNA expression profile

Expression levels of miR-96 and miR-96* in a panel of RNAs from human (First Choice total RNA; Ambion, Austin, TX, USA) and adult mouse tissues were evaluated by semi-quantitative real-time RT–PCR, using specific assays (Supplementary Material, Table S2). The organs of Corti from wild-type P4 mice (background 129S5) were kindly provided by prof. Karen Steel (Wellcome Trust Sanger Institute, Hinxton, UK). Total RNA extraction was performed as reported (15), and first-strand cDNA synthesis was carried out as described above. All assays were performed in triplicate on a LightCycler 480 (Roche), using a touch-down thermal profile (PCR conditions are available on request). MiRNAs expression levels were quantified by the △△CT method using either the U6 RNA (human) or the snoRNA 142 (mouse) as internal normalization reference.

SUPPLEMENTARY MATERIAL

Supplementary Material is available at *HMG* online.

ACKNOWLEDGEMENTS

We are indebted to all study subjects for their participation, without whom this research would be impossible. Chiara Radaelli, Francesca Balistreri and Ileana Guerrini are acknowledged for their invaluable assistance and technical support.

Conflict of Interest statement. None declared.

FUNDING

This work was supported by PUR 10% (Programma dell'Università per la Ricerca) 2009 from the Università degli Studi di Milano and by the Italian Telethon Foundation, Grant number GGP11177. Funding to pay the Open Access publication charges for this article was provided by the Italian Telethon Foundation.

REFERENCES

1. Huntzinger, E. and Izaurralde, E. (2011) Gene silencing by microRNAs: contributions of translational repression and mRNA decay. *Nat. Rev. Genet.*, **12**, 99–110.
2. Bartel, D.P. (2009) MicroRNAs: target recognition and regulatory functions. *Cell*, **136**, 215–233.
3. Krol, J., Loedige, I. and Filipowicz, W. (2010) The widespread regulation of microRNA biogenesis, function and decay. *Nat. Rev. Genet.*, **11**, 597–610.
4. Ro, S., Park, C., Young, D., Sanders, K.M. and Yan, W. (2007) Tissue-dependent paired expression of miRNAs. *Nucleic Acids Res.*, **35**, 5944–5953.
5. Okamura, K., Phillips, M., Tyler, D., Duan, H., Chou, Y. and Lai, E. (2008) The regulatory activity of microRNA* species has substantial influence on microRNA and 3′ UTR evolution. *Nat. Struct. Mol. Biol.*, **15**, 354–363.
6. de Wit, E., Linsen, S.E., Cuppen, E. and Berezikov, E. (2009) Repertoire and evolution of miRNA genes in four divergent nematode species. *Genome Res.*, **19**, 2064–2074.
7. Marco, A., Hui, J.H., Ronshaugen, M. and Griffiths-Jones, S. (2010) Functional shifts in insect microRNA evolution. *Genome Biol. Evol.*, **2**, 686–696.
8. Yang, J.S., Phillips, M.D., Betel, D., Mu, P., Ventura, A., Siepel, A.C., Chen, K.C. and Lai, E.C. (2011) Widespread regulatory activity of vertebrate microRNA* species. *RNA*, **17**, 312–326.
9. Pierce, M., Weston, M., Fritzsch, B., Gabel, H., Ruvkun, G. and Soukup, G. (2008) MicroRNA-183 family conservation and ciliated neurosensory organ expression. *Evol. Dev.*, **10**, 106–113.
10. Soukup, G., Fritzsch, B., Pierce, M., Weston, M., Jahan, I., McManus, M. and Harfe, B. (2009) Residual microRNA expression dictates the extent of inner ear development in conditional Dicer knockout mice. *Dev. Biol.*, **328**, 328–341.
11. Li, H., Kloosterman, W. and Fekete, D. (2010) MicroRNA-183 family members regulate sensorineural fates in the inner ear. *J. Neurosci.*, **30**, 3254–3263.

12. Kapsimali, M., Kloosterman, W., de Bruijn, E., Rosa, F., Plasterk, R. and Wilson, S. (2007) MicroRNAs show a wide diversity of expression profiles in the developing and mature central nervous system. *Genome Biol.*, **8**, R173.
13. Friedman, L. and Avraham, K. (2009) MicroRNAs and epigenetic regulation in the mammalian inner ear: implications for deafness. *Mamm. Genome*, **9–10**, 581–603.
14. Mencía, A., Modamio-Høybjør, S., Redshaw, N., Morín, M., Mayo-Merino, F., Olavarrieta, L., Aguirre, L., del Castillo, I., Steel, K., Dalmay, T. *et al.* (2009) Mutations in the seed region of human miR-96 are responsible for nonsyndromic progressive hearing loss. *Nat. Genet.*, **41**, 609–613.
15. Lewis, M., Quint, E., Glazier, A., Fuchs, H., De Angelis, M., Langford, C., van Dongen, S., Abreu-Goodger, C., Piipari, M., Redshaw, N. *et al.* (2009) An ENU-induced mutation of miR-96 associated with progressive hearing loss in mice. *Nat. Genet.*, **41**, 614–618.
16. Kuhn, S., Johnson, S.L., Furness, D.N., Chen, J., Ingham, N., Hilton, J.M., Steffes, G., Lewis, M.A., Zampini, V., Hackney, C.M. *et al.* (2011) miR-96 regulates the progression of differentiation in mammalian cochlear inner and outer hair cells. *Proc. Natl Acad. Sci. USA*, **108**, 2355–2360.
17. Hildebrand, M., Witmer, P., Xu, S., Newton, S., Kahrizi, K., Najmabadi, H., Valle, D. and Smith, R. (2010) miRNA mutations are not a common cause of deafness. *Am. J. Med. Genet. A*, **152A**, 646–652.
18. Soares, A., Pereira, P., Santos, B., Egas, C., Gomes, A., Arrais, J., Oliveira, J., Moura, G. and Santos, M. (2009) Parallel DNA pyrosequencing unveils new zebrafish microRNAs. *BMC Genomics*, **10**, 195.
19. Zuker, M. (2003) Mfold web server for nucleic acid folding and hybridization prediction. *Nucleic Acids Res.*, **31**, 3406–3415.
20. Kertesz, M., Iovino, N., Unnerstall, U., Gaul, U. and Segal, E. (2007) The role of site accessibility in microRNA target recognition. *Nat. Genet.*, **39**, 1278–1284.
21. Krüger, J. and Rehmsmeier, M. (2006) RNAhybrid: microRNA target prediction easy, fast and flexible. *Nucleic Acids Res.*, **34**, W451–W454.
22. Betel, D., Koppal, A., Agius, P., Sander, C. and Leslie, C. (2010) Comprehensive modeling of microRNA targets predicts functional non-conserved and non-canonical sites. *Genome Biol.*, **11**, R90.
23. Duan, R., Pak, C. and Jin, P. (2007) Single nucleotide polymorphism associated with mature miR-125a alters the processing of pri-miRNA. *Hum. Mol. Genet.*, **16**, 1124–1131.
24. Sun, G., Yan, J., Noltner, K., Feng, J., Li, H., Sarkis, D.A., Sommer, S.S. and Rossi, J.J. (2009) SNPs in human miRNA genes affect biogenesis and function. *RNA*, **15**, 1640–1651.
25. Jazdzewski, K., Murray, E.L., Franssila, K., Jarzab, B., Schoenberg, D.R. and de la Chapelle, A. (2008) Common SNP in pre-miR-146a decreases mature miR expression and predisposes to papillary thyroid carcinoma. *Proc. Natl Acad. Sci. USA*, **105**, 7269–7274.
26. Jazdzewski, K., Liyanarachchi, S., Swierniak, M., Pachucki, J., Ringel, M.D., Jarzab, B. and de la Chapelle, A. (2009) Polymorphic mature microRNAs from passenger strand of pre-miR-146a contribute to thyroid cancer. *Proc. Natl Acad. Sci. USA*, **106**, 1502–1505.
27. Guella, I., Pistocchi, A., Asselta, R., Rimoldi, V., Ghilardi, A., Sironi, F., Trotta, L., Primignani, P., Zini, M., Zecchinelli, A. *et al.* (2010) Mutational screening and zebrafish functional analysis of GIGYF2 as a Parkinson-disease gene. *Neurobiol. Aging*, **11**, 1994–2005.
28. Nielsen, C.B., Shomron, N., Sandberg, R., Hornstein, E., Kitzman, J. and Burge, C.B. (2007) Determinants of targeting by endogenous and exogenous microRNAs and siRNAs. *RNA*, **13**, 1894–1910.
29. May-Simera, H.L., Ross, A., Rix, S., Forge, A., Beales, P.L. and Jagger, D.J. (2009) Patterns of expression of Bardet-Biedl syndrome proteins in the mammalian cochlea suggest noncentrosomal functions. *J. Comp. Neurol.*, **514**, 174–188.
30. Mothe, A.J. and Brown, I.R. (2001) Expression of mRNA encoding extracellular matrix glycoproteins SPARC and SC1 is temporally and spatially regulated in the developing cochlea of the rat inner ear. *Hear. Res.*, **155**, 161–174.
31. McCullar, J.S., Ty, S., Campbell, S. and Oesterle, E.C. (2010) Activin potentiates proliferation in mature avian auditory sensory epithelium. *J. Neurosci.*, **30**, 478–490.
32. Kuhn, S., Knirsch, M., Rüttiger, L., Kasperek, S., Winter, H., Freichel, M., Flockerzi, V., Knipper, M. and Engel, J. (2009) Ba2+ currents in inner and outer hair cells of mice lacking the voltage-dependent Ca2+ channel subunits beta3 or beta4. *Channels*, **3**, 366–376.
33. Robertson, N.G., Khetarpal, U., Gutiérrez-Espeleta, G.A., Bieber, F.R. and Morton, C.C. (1994) Isolation of novel and known genes from a human fetal cochlear cDNA library using subtractive hybridization and differential screening. *Genomics*, **23**, 42–50.
34. Daudet, N. and Lebart, M.C. (2002) Transient expression of the t-isoform of plastins/fimbrin in the stereocilia of developing auditory hair cells. *Cell Motil. Cytoskeleton*, **53**, 326–336.
35. Denti, M.A., Rosa, A., Sthandier, O., De Angelis, F.G. and Bozzoni, I. (2004) A new vector, based on the PolII promoter of the U1 snRNA gene, for the expression of siRNAs in mammalian cells. *Mol. Ther.*, **10**, 191–199.
36. Livak, K.J. and Schmittgen, T.D. (2001) Analysis of relative gene expression data using real-time quantitative PCR and the 2(-Delta Delta C(T)) Method. *Methods*, **25**, 402–408.